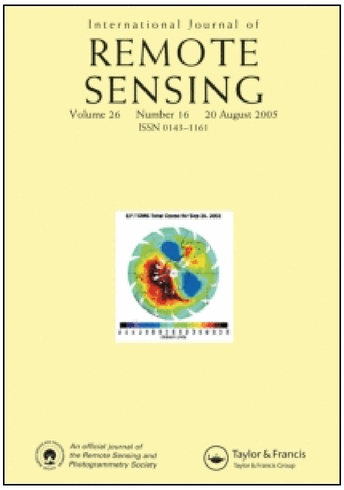

International Journal of Remote Sensing
Publication details, including instructions for authors and subscription information:
http://www.informaworld.com/smpp/title~content=t713722504

Kuroshio variations in the upstream region as seen by HF radar and satellite altimetry data

K. Ichikawa [ab]; R. Tokeshi [c]; M. Kashima [d]; K. Sato [d]; T. Matsuoka [d]; S. Kojima [d]; S. Fujii [de]
[a] Research Institute for Applied Mechanics, Kyushu University, Kasuga, 816-8580 Japan [b] Institute of Observational Research for Global Change, Japan Agency for Marine-Earth Science and Technology, Yokosuka, 237-0061 Japan [c] Interdisciplinary Graduate School of Engineering Sciences, Kyushu University, Kasuga, 816-8580 Japan [d] National Institute of Information and Communications Technology, 4484 Onna, Kunigami, 904-0411 Japan [e] Faculty of Engineering, University of Ryukyus, Nishihara, 903-0213 Japan

Online Publication Date: 01 November 2008

International Journal of Remote Sensing
Vol. 29, No. 21, 10 November 2008, 6417–6426

Taylor & Francis
Taylor & Francis Group

Kuroshio variations in the upstream region as seen by HF radar and satellite altimetry data

K. ICHIKAWA*†‡, R. TOKESHI§, M. KASHIMA¶, K. SATO¶, T. MATSUOKA¶, S. KOJIMA¶ and S. FUJII¶**

†Research Institute for Applied Mechanics, Kyushu University, Kasuga, 816–8580 Japan

‡Institute of Observational Research for Global Change, Japan Agency for Marine-Earth Science and Technology, Yokosuka, 237-0061 Japan

§Interdisciplinary Graduate School of Engineering Sciences, Kyushu University, Kasuga, 816-8580 Japan

¶National Institute of Information and Communications Technology, 4484 Onna, Kunigami, 904-0411 Japan

**Faculty of Engineering, University of Ryukyus, Nishihara, 903-0213 Japan

(*Received 2 May 2007; in final form 5 November 2007*)

Variations of the position and speed of the Kuroshio are studied by a combination of high-resolution high-frequency (HF) ocean radar data and wide-coverage altimetry data. The speed of the Kuroshio and its position are determined along 123.35° E northeast of Taiwan from daily maps of surface geostrophic velocity estimated from HF radar data from August 2001 to February 2005. These two are found to be well correlated for mesoscale variations with periods of a few months, as the Kuroshio tends to be faster (or slower) when its axis moves south (or north). This tendency is significant in summer when the Kuroshio is seasonally intensified and well-defined in the HF radar data. By taking correlation with the sea surface dynamic height anomaly observed by satellite altimeters, these Kuroshio variations in the East China Sea are found to be induced by merging of mesoscale eddies from the east at 21° N and by coincident Kuroshio meanders east of Taiwan.

1. Introduction

Understanding of mesoscale variability in the ocean currents has been significantly improved by the use of satellite altimetry. In the upstream region of the Kuroshio, for example, westward-propagating mesoscale eddies observed by satellite altimetry are found to be strongly related to variations of the Kuroshio volume transport obtained by moored current meters along the World Ocean Circulation Experiment (WOCE) PCM–1 observation line east of Taiwan (Lee *et al.* 2001). Furthermore, increase (or decrease) of the Kuroshio volume transport in the Tokara Strait determined by tide gauge records is found to be well correlated with merging of anticyclonic (or cyclonic) mesoscale eddies upstream of the Kuroshio (northeast of Taiwan and south of Okinawa) approximately 30 days before (Ichikawa 2001).

*Corresponding author. Email: ichikawa@riam.kyushu-u.ac.jp

International Journal of Remote Sensing
ISSN 0143-1161 print/ISSN 1366-5901 online
http://www.tandf.co.uk/journals
DOI: 10.1080/01431160802175454

It should be noted, however, that those new findings of the Kuroshio fluctuations are obtained based not only on observations of mesoscale eddies by satellite altimetry but also indexes of the Kuroshio variations determined from observations other than altimetry. Since maps of the sea surface dynamic height anomaly (SSDHA) field are generally interpolated using along-track altimetry data for a period longer than 10 days (repeat cycle of an altimeter) with spatial and temporal smoothing, such fast-moving phenomena as meanders of the Kuroshio cannot be resolved well with these maps alone (Ichikawa *et al.* 1995). Moreover, temporal anomaly does not describe adequately the variations of the Kuroshio having a strong mean component (Ichikawa and Imawaki 1994). In other words, observations other than satellite altimetry data are necessary to observe variations of the Kuroshio themselves, even though the altimetry is very efficient to investigate surrounding oceanographic conditions that would induce the variations of the Kuroshio.

Since July 2001, sea surface currents in the upstream region of the Kuroshio have been monitored by the high-frequency ocean radar (hereafter HF radar) system developed by the National Institute of Information and Communications Technology (NICT), Japan. HF radar measures the sea surface velocity component in the direction toward the radar, using the Doppler frequency shift of the radio wave backscattered by ocean surface wind waves within an observation cell (footprint) of the radar (e.g., Stewart and Joy 1974); the vector velocity is determined by combining observed radial velocity components of two (or more) radars. Since the HF radar data have higher resolution in space and time than satellite altimetry and they are not confined to a temporal anomaly, the HF radar system is considered to be more suitable to observe fast-propagating disturbances of the Kuroshio in the limited observation area. Recently, Tokeshi *et al.* (2007) has established a method to remove ageostrophic components in the HF radar observations such as the wind-driven Ekman current, tidal currents and inertial oscillations. Combined use of geostrophic velocity observations by the HF radar and satellite altimeters could provide a comprehensive description of the variations of the Kuroshio in the upstream region.

In this study, therefore, we first describe variations of the position and speed of the Kuroshio in the upstream region that are determined from time series of the HF geostrophic velocity in §3. Then, their correlation with the surrounding SSDHA is studied in §4, in order to investigate possible factors that would cause variations of the Kuroshio. Discussions on these results will be given in §5 together with a brief summary, while the data used in this study are described in §2.

2. Data

Each HF radar, placed on Ishigaki and Yonaguni Islands (figure 1), measures the radial surface velocity component at 7-km and 0.5-hour intervals (Matsuoka *et al.* 2003, Sato *et al.* 2004). We use 3.5 years of gridded vector velocity data from July 2001 to January 2005, which are produced by NICT on a 7-km grid every 0.5 hours from those radial velocities. The tidal current component of nine constituents (M_2, S_2, N_2, K_2, K_1, O_1, P_1, Q_1 and M_f) determined by harmonic analysis is first removed and then the daily-mean HF velocity field is determined. Then, the wind-driven Ekman current component estimated from the satellite-borne daily-mean wind (CERSAT 2002) by Tokeshi *et al.* (2007) is removed. Finally, the velocity data are further smoothed over three days in order to reduce the residual ageostrophic component such as inertial oscillations (Tokeshi *et al.* 2007).

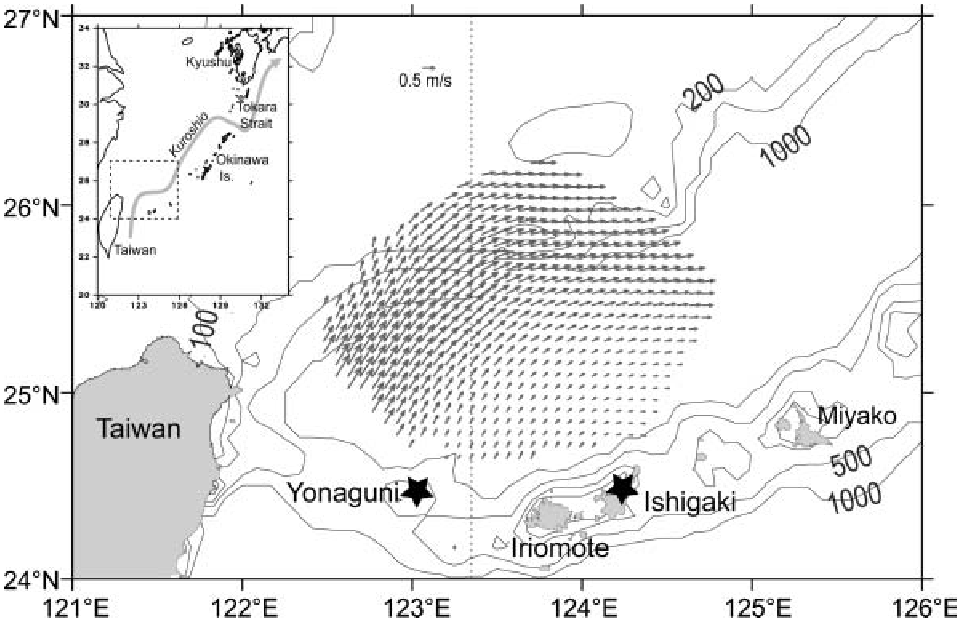

Figure 1. The 3.5-year averaged surface velocity in the upstream of the Kuroshio superimposed on the bathymetry contours (100, 200, 500 and 1000 m); the study area is indicated by a dashed square in a wider schematic map at the top left corner. The star marks show the position of the HF radars, on Ishigaki and Yonaguni Islands. The reference velocity of $0.5\,\mathrm{m\,s^{-1}}$ is also plotted at the top. The meridional line at 123.35° E is also plotted by a dotted line for further reference.

Along-track altimetry data sets of TOPEX/POSEIDON (T/P), Jason-1, ERS-2 and Envisat used in the present study were produced by SSALTO/DUACS and distributed by AVISO with support from CNES as the delayed time data (AVISO 2004). From all these altimetry data, the SSDHA field is determined on a 0.25-degree grid by an optimal interpolation every 9.92 days (a repeat cycle of T/P). The optimal interpolation used in the present study is the same as that described by Ichikawa *et al.* (2004), except replacing the data sets by the extended ones; note that spatial and temporal smoothing scales used in the optimal interpolation are approximately 70 km and 35 days, respectively, so that signals with scales smaller than these are reduced in the estimated SSDHA field.

3. Variations of the Kuroshio

In order to investigate variations of the Kuroshio in the upstream region, we first need to define some indexes of the Kuroshio variations in the HF radar data. Assuming that the Kuroshio always crosses the meridional line at 123.35° E, near the centre of the HF observational area shown in figure 1, we characterize the speed of the Kuroshio simply as the maximum speed of the daily HF geostrophic velocity along 123.35° E, and the position of the Kuroshio axis as the latitude of the maximum speed. Furthermore, approximate positions of the northern and southern boundaries of the Kuroshio are also determined as boundaries of a band of the area around the estimated Kuroshio axis in which the speed exceeds $0.5\,\mathrm{m\,s^{-1}}$. Probable problems related with these simple definitions will be discussed in §5.

Variations of those indexes are plotted in figure 2, which consist of fluctuations with various frequencies. Among them, long-term variations of the Kuroshio speed

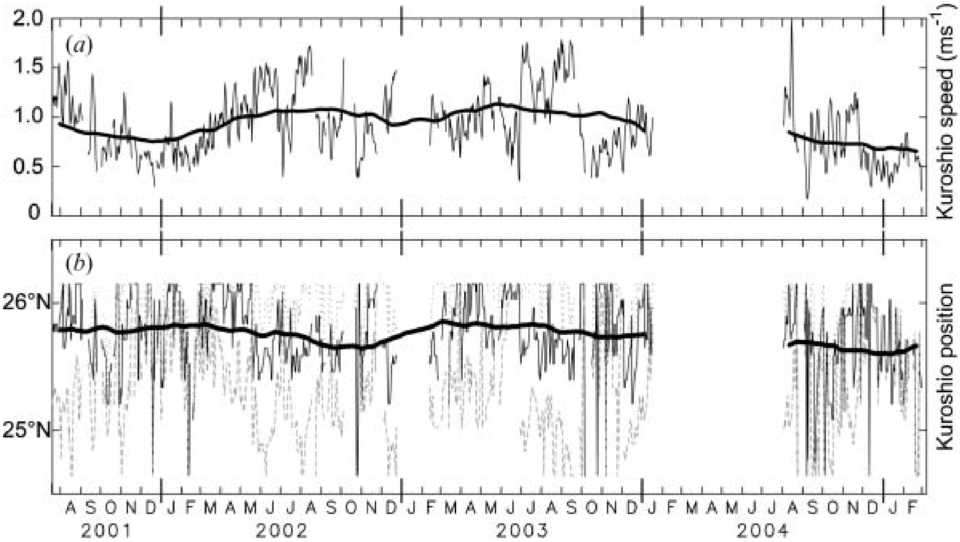

Figure 2. Time series of the Kuroshio speed (*a*) and the Kuroshio position (*b*). Bold lines indicate 240-day averaged data. Southern and northern boundaries of the areas where the speed exceeds $0.5\,\mathrm{m\,s^{-1}}$ are also plotted in the lower panel (*b*) by dashed and dotted lines, respectively.

(longer than 240 days) show seasonality; namely, the Kuroshio speed tends to be slower in winter and faster in summer with an order of 0.2–$0.3\,\mathrm{m\,s^{-1}}$ difference (figure 2*a*). Consequently, the width of the Kuroshio also shows seasonal variations (figure 2*b*); the width (or distance between the northern and southern boundaries) increases up to approximately 150 km in summer, but may decrease to 0 km by definition when the Kuroshio speed is less than $0.5\,\mathrm{m\,s^{-1}}$ in winter. Note that this definition might be misleading since the weaker Kuroshio tends to be broader in general with less horizontal velocity shear. Meanwhile, seasonal variations are not significant for the Kuroshio position (figure 2*b*), although the Kuroshio seems to shift slightly southward in autumn by approximately 0.1°.

Mesoscale variations with periods shorter than 240 days but longer than 10 days are extracted in figure 3. Dominant periods for the mesoscale variations are a few months for both speed and position of the Kuroshio. The amplitude of such mesoscale variations of the Kuroshio speed reaches up to $0.5\,\mathrm{m\,s^{-1}}$ in summer, although it decreases to less than $0.2\,\mathrm{m\,s^{-1}}$ in winter and spring (figure 3*a*). On the contrary, the mesoscale variations of the Kuroshio position are more (or less) prominent in winter (or summer), as seen in figure 3(*b*).

Unlike the long-term variations in figure 2, these mesoscale variations of the Kuroshio position in figure 3(*b*) are generally in phase with those of the Kuroshio speed in figure 3(*a*). Namely, the Kuroshio tends to move northward (or southward) when the speed of the Kuroshio is slower (or faster). This simultaneity is especially obvious in summer (e.g., from June to September) but less significant in winter, as partially suggested in previous studies (Tang *et al.* 2000). These results will be discussed in §5.

4. Correlation with surrounding SSDHA

The upper panels of figure 4 show examples of the HF geostrophic velocity field in summer 2003 when large mesoscale variations are present in figure 3. As seen in

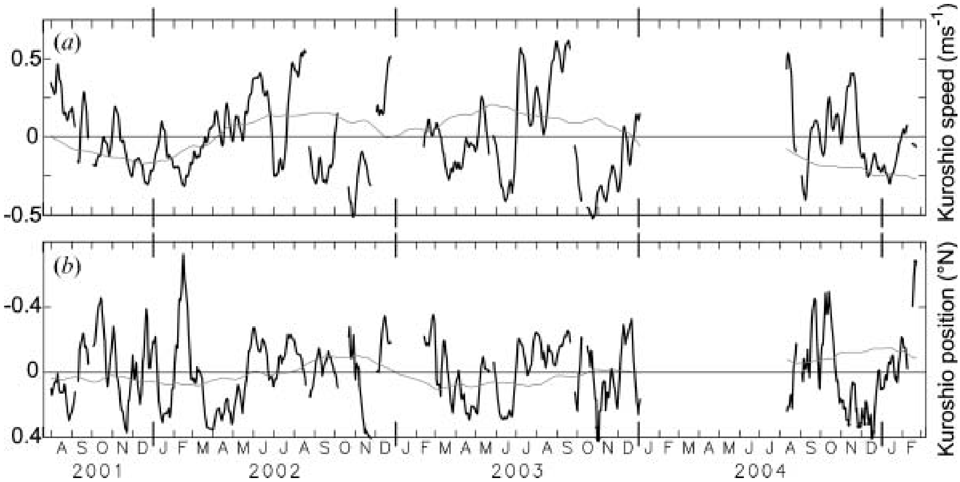

Figure 3. As figure 2, but for mesoscale fluctuations which are band-passed with periods from 10 to 240 days. Thin lines indicate 240-day averaged data shown in figure 2. Note that southward shifts are plotted upward in the lower panel (*b*) for convenience.

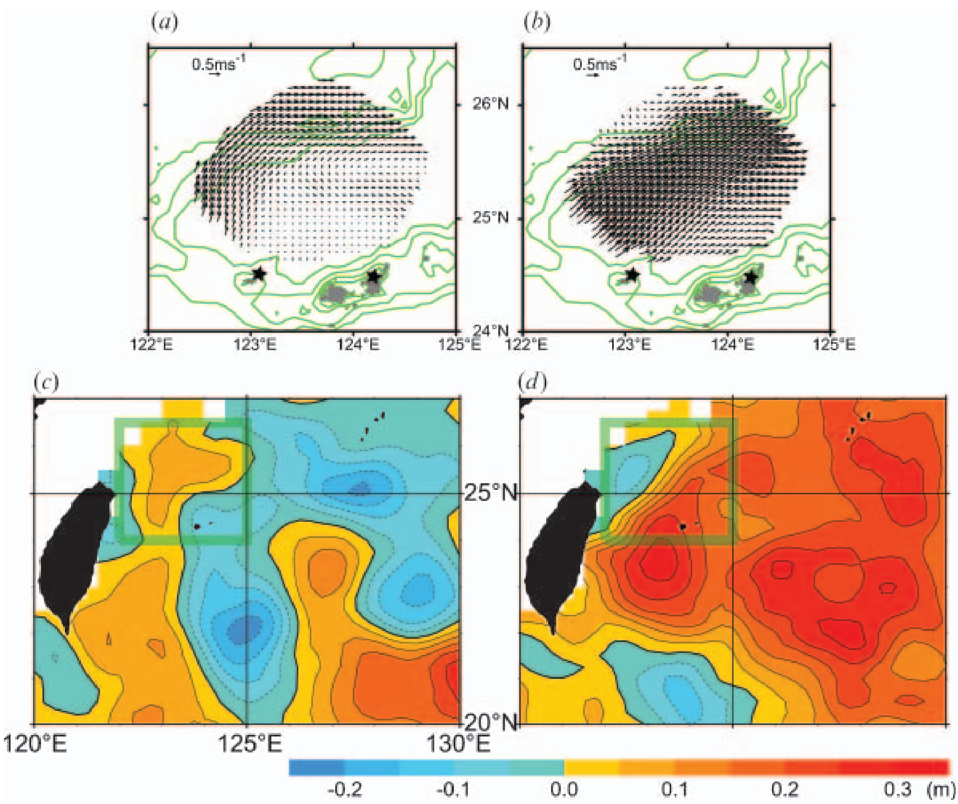

Figure 4. The HF velocity maps on 1 June 2003 (*a*) and 13 September 2003 (*b*), and the SSDHA maps on 30 May 2003 (*c*) and 7 September 2003 (*d*). The star marks and the bathymetry contours shown by green lines in the upper panels are the same as figure 1. In the lower panels, contour intervals are 0.05 m and green boxes indicate an area of the upper panels.

figure 2, the weaker Kuroshio moved north of 26° N to be located on the continental shelf in June (figure 4*a*), while in September, a wide band of faster speed with large meridional shear was situated along the south of the slope (figure 4*b*).

Corresponding SSDHA maps are plotted as the lower panels of figure 4. In both panels figures 4(*c*) and 4(*d*), pairs of positive and negative SSDHA areas are found near the northwest and southeast corners of the green boxes that indicate the area of the upper panels, but the signs are opposite in figures 4(*c*) and 4(*d*). Namely, a positive (or negative) SSDHA area was present near the northwest corner and negative (or positive) one near the southeast corner for the weaker and northern (or stronger and southern) Kuroshio in figure 4(*c*) (or 4*d*). Considering the spatial gradient of the SSDHA, this pair of SSDHAs indicates the presence of a southwestward (or northeastward) geostrophic velocity anomaly at nearly the centre of the HF observation area in figure 4(*c*) (or 4*d*). The directions of these geostrophic velocity anomalies are consistent with the weakening and strengthening of the Kuroshio, although the magnitude of the geostrophic velocity anomaly in the lower panels would not be sufficiently large to explain the HF velocity differences in the upper panels; this would be probably due to spatial smoothing of the gridded SSDHA when it was interpolated.

In addition to the SSDHA distribution within the HF observation area, noticeable mesoscale SSDHA eddies are also present in the surrounding area. Especially, upstream mesoscale eddies east of Taiwan at 22°–23.5° N are connected to the SSDHA in the southeastern part of the HF observation area described above.

In order to understand the oceanographic conditions that induce variations of the Kuroshio, we took a correlation between the mesoscale variations of the Kuroshio speed in figure 3(*a*) and a time series of the surrounding SSDHA. The Kuroshio speed is first averaged over the same 10 days to match up with the SSDHA data resolution, then a correlation coefficient is calculated at each grid point with the SSDHA on the corresponding date, and also with the SSDHA 20 and 40 days before.

As expected from figure 4, a pair of positive and negative significant correlations is found in the northwest and southeast corners of the HF observation area shown by a green box when no temporal lags are accounted for (figure 5*c*). The area of positive correlation in figure 5(*c*) is centred at 24° N, 123.5° E near Yonaguni and Iriomote Islands, while it is located at 21°–23° N east of Taiwan when correlation is

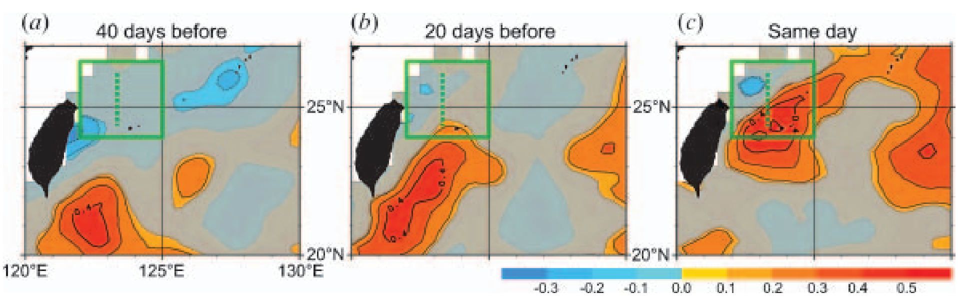

Figure 5. Distribution of correlation coefficients between the mesoscale variations of the Kuroshio speed in figure 3(*a*) and the SSDHA 40 days before (*a*), 20 days before (*b*), and on the same day (*c*). Contour intervals are 0.1 and areas are masked with confidence level less than 90% by Fisher's *z*-test (Press *et al.* 1992). Green boxes are the same as figure 4. Broken green lines in the boxes indicate 123.35° E where the Kuroshio speed is defined.

taken with the SSDHA 20 days before (figure 5*b*), and at 21° N southeast of Taiwan with the SSDHA 40 days before (figure 5*a*). The successive displacement of the positive correlation areas with temporal lags suggests that positive (or negative) SSDHA mesoscale eddies at 21° N would eventually induce an increase (or decrease) of the Kuroshio speed downstream in the East China Sea 40 days later.

Meanwhile, the negative correlation centred at 25.5° N, 122.5° E on the continental shelf in figure 5(*c*) can also be recognized shifted as the temporal lag changes. An area of significant negative correlation is evidently present along the east coast of Taiwan at 24° N in figure 5(*a*), while in figure 5(*b*), two areas of negative correlation are found; one is located at almost the same position in figure 5(*c*), and another at 24.5° N, 122° E at the northeast edge of Taiwan, downstream of the centre position in figure 5(*a*). Although the correlations in figure 5(b) are weak and separated, all those negative correlations in figure 5 would represent successive displacements, accounting that some parts of fast-moving small-scale signals tend to be lost in the gridded SSDHA data (Ichikawa 2001). Therefore, apart from the mesoscale eddies at 21° N, SSDHA signals propagating along the east coast of Taiwan and the continental shelf edge are also correlated negatively with the mesoscale variation of the Kuroshio speed in the East China Sea.

From analysis of WOCE PCM–1 observation data, satellite altimetry data and trajectory data of surface drifters, Zhang *et al.* (2001) concluded that negative SSDHAs along the east coast of Taiwan of approximately 100-day temporal scales are relevant to seaward Kuroshio meanders. If the seaward meanders of the Kuroshio east of Taiwan propagate downstream as the negative correlation area in figure 5, a southward shift of the Kuroshio in the East China Sea would be expected approximately 40 days later, coincidentally with an increase of the Kuroshio speed. This is consistent with our results in the previous section that a southward (or northward) shift of the Kuroshio at 123.35° E is coincident with an increase (or decrease) of the Kuroshio speed. It should also be noticed that Zhang *et al.* (2001) additionally suggested that westward-propagating anticyclonic eddies between 18° N and 23° N would force a large seaward Kuroshio shift east of Taiwan. This would also explain the coincident presence of the positive correlation at 21° N and the negative correlation at 24° N in figure 5(*a*).

5. Summary and discussions

Using spatio-temporally high-resolution HF radar geostrophic velocity data in the upstream region (figure 1), variations of the speed and position of the Kuroshio have been determined along the 123.35° E meridional line. A seasonal change is recognized in the Kuroshio speed variations, being faster in summer and slower in winter (figure 2*a*). The decrease of eastward current in winter might be caused by insufficient removal of the wind-driven Ekman current in winter, whose direction would be westward. However, weakening (or strengthening) of the Kuroshio in the East China Sea in winter (or summer) has been often reported, at least qualitatively, in previous studies (e.g., Ichikawa and Beardsley 1993, Lee *et al.* 2001).

By definition in this study, the width of the Kuroshio, or a band of an area in which the speed exceeds $0.5\,\mathrm{m\,s^{-1}}$, corresponds to the seasonal variations of the Kuroshio speed. Meanwhile, seasonal signals are not significant in variations of the position of the Kuroshio axis (figure 2*b*). However, it should be noted that variations of the northern boundary of the Kuroshio in figure 2(*b*) are not as fully described as those of the southern boundary, due to limitation of the HF observation area. This limitation may contaminate quantitative discussions of the Kuroshio position and width, especially when the Kuroshio axis moves far north, as in late March 2002; for example, the northern part of the Kuroshio shown in figure 4(*a*) does not seem fully observed. Moreover, the simple definition of the Kuroshio axis adopted in this study (the position of the maximum speed along the meridional line) would introduce an inherent problem when the Kuroshio speed is slow. The speed at the Kuroshio axis would be singularly large when the Kuroshio is strong, so that the position of the Kuroshio axis is less sensitive to small changes of the speed near the axis due to large velocity shear across the Kuroshio as in figure 4(*b*). Meanwhile, the speed around the Kuroshio axis would become more similar to that of the Kuroshio axis if the Kuroshio is weak and broad as in figure 4(*a*), so that a slight difference of the speed would cause a large shift of the position of the maximum speed. In other words, the position of the Kuroshio could be largely affected by observational errors of the HF radar when the Kuroshio is weak. In addition, the presence of a significant offshore mesoscale eddy may cause a pseudo-rapid southward shift of the axis if the Kuroshio is relatively weaker, as in February 2002 in figures 2(*b*) and 3(*b*). Therefore, more rational definitions of the Kuroshio axis and width would be necessary for further study, such as in Ambe *et al.* (2004). Note that the inherent sensitivity of the Kuroshio position would also explain the larger (or smaller) amplitude of the mesoscale variations of the Kuroshio position in winter (or summer) in figure 3(*b*) when the horizontal velocity shear across the Kuroshio tends to be smaller (or larger).

Actually, a southward (or northward) shift of the Kuroshio axis in summer (or winter) has been reported in previous studies (e.g., Chern and Wang 1994, Tang *et al.* 2000), which would support unreliability of the present estimates of the Kuroshio position in winter when the Kuroshio is weaker and when the axis moves northwards. Note that Tang *et al.* (2000) also reported the coincident presence of a cyclonic eddy centred around Mien-Hua Canyon (25.4° N, 122.4° E) when the Kuroshio shifts southward in summer. Consequently, the southern and stronger Kuroshio in summer is considered to accompany an area of negative SSDHA on the continental shelf where negative correlation is found in figure 5(*c*). Such a similarity to the mesoscale variations in figure 5 suggests that the seasonal Kuroshio variations would also be induced by merging of upstream offshore eddies into the Kuroshio. For quantitative discussions, however, further studies are necessary with improved indexes of the seasonal Kuroshio variations.

Most significant mesoscale variations both for the Kuroshio speed and the Kuroshio position have periods of a few months, which are equivalent to 100 days suggested in previous studies (Yang *et al.* 1999, Zhang *et al.* 2001). Mesoscale variations of the Kuroshio speed are simultaneous with those of the Kuroshio position, especially in summer when their estimations are more reliable as mentioned above. Namely, the Kuroshio moves northward (or southward) when the Kuroshio is stronger (or weaker). By taking temporally lagged correlation with the SSDHA, the mesoscale variations of the Kuroshio speed at 123.35° E are found to be induced by mesoscale eddies merged into the Kuroshio at 21° N that propagate downstream accompanied with meanders of the Kuroshio (figure 5). These results suggest successive phenomena as follows: a mesoscale eddy with positive (or negative) SSDHA at 21° N approaching from the east to the Kuroshio induces seaward (or coastward) meander of the Kuroshio east of Taiwan, following anticyclonic (or cyclonic) rotation of the eddy. Then the mesoscale eddy merges into the Kuroshio and starts to propagate downstream together with the meander. Approximately 40 days later, the seaward (or coastward) meander reaches the HF observation area, with coincident increase (or decrease) of the Kuroshio speed due to the offshore positive (or negative) SSDHA originated from the merged mesoscale eddy.

These results are quantitatively independent of the choices of the reference lines, either along meridional lines at different longitudes or along oblique northwest–southeast lines (Matsuoka *et al.* 2003, Kojima and Sato 2007). Since meanders of the Kuroshio propagate fast, no difference would be recognized within the HF observation area for variations with periods longer than 10 days discussed in this paper. For small-scale events such as growth of meanders, however, discussions using higher-resolution HF data would be necessary to focus on the ageostrophic components including their convergence or divergence, although they are outside of the scope of this paper.

Acknowledgments

This work is part of a project called 'Monitoring and prediction of marine and atmospheric environmental changes in East Asia' of the Research Institute for Applied Mechanics, Kyushu University. This paper is also partially sponsored by the Hydrospheric Atmospheric Research Center, Nagoya University, as part of collaborative research programs.

References

AMBE, D., IMAWAKI, S., UCHIDA, H. and ICHIKAWA, K., 2004, Estimating the Kuroshio axis south of Japan using combination of satellite altimetry and drifting buoys. *Journal of Oceanography*, **60**, pp. 375–382.

AVISO, 2004, Ssalto/Duacs User Handbook: (M)SLA and (M)ADT Near-Real Time and Delayed Time Products, SALP-MU-P-EA-21065-CLS, Edition 1.2.

CERSAT, 2002, QUIKSCAT Scatterometer Mean Wind Field Products User Manual. C2-MUT-W-03-IF, Ver.1.0.

CHERN, C.-S. and WANG, J., 1994, Influence of the seasonal thermocline on the intrusion of Kuroshio across the continental shelf northeast of Taiwan. *Journal of Oceanography*, **50**, pp. 691–711.

ICHIKAWA, H. and BEARDSLEY, R.C., 1993, Temporal and spatial variability of volume transport of the Kuroshio in the East China Sea. *Deep Sea Resarch Part I*, **40**, pp. 583–605.

ICHIKAWA, K. and IMAWAKI, S., 1994, Life history of a cyclonic ring detached from the Kuroshio Extension as seen by the Geosat altimeter. *Journal of Geophysical Research*, **99**, pp. 15953–15966.

ICHIKAWA, K., IMAWAKI, S. and ISHII, H., 1995, Comparison of surface velocities determined from altimeter and drifting buoy data. *Journal of Oceanography*, **51**, pp. 729–740.

ICHIKAWA, K., 2001, Variation of the Kuroshio in the Tokara Strait induced by meso-scale eddies. *Journal of Oceanography*, **57**, pp. 55–68.

ICHIKAWA, K., GOHDA, N., ARAI, M. and KANEKO, A., 2004, Monitoring surface velocity from repeated ADCP observations and satellite altimetry. *Jounal of Oceanography*, **60**, pp. 365–374.

KOJIMA, S. and SATO, K., 2007, Observation of the Kuroshio current in southwest East China Sea by long-range ocean radar. *Proceedings of the 30th International Conference on Coastal Engineering 2006*, pp. 1306–1316.

LEE, T.N., JOHNS, W.E., LIU, C.-T., ZHANG, D.X., ZANTOPP, R. and YANG, Y., 2001, Mean transport and seasonal cycle of the Kuroshio east of Taiwan with comparison to the Florida Current. *Journal of Geophysical Research*, **106**, pp. 22143–22158.

MATUOKA, T., KENJI, S., KOJIMA, S. and FUJII, S., 2003, HF ocean radar observation of surface currents induced by a typhoon in the East China Sea. *IEEE Proceedings of International Geoscience and Remote Sensing Symposium 2003*, I-F05-03.

PRESS, W.H., TEUKOLSKY, S.A., VETTERLING, W.T. and FLANNERY, B.P., 1992, Numerical Recipes in FORTRAN; the art of scientific computing, 2nd ed. Cambridge University Press.

SATO, K., MATSUOKA, T., KOJIMA, S. and FUJII, S., 2004, Long-range ocean radar observation of Kuroshio upstream region in the East China Sea. *Bulletin of Coastal Oceanography*, **41**, pp. 119–127 (in Japanese with English abstract).

STEWART, R.H. and JOY, J.W., 1974, HF radio measurements of surface currents. *Deep-Sea Research*, **21**, pp. 1039–1049.

TANG, T.Y., TAI, J.H. and YANG, T.J., 2000, The flow pattern north of Taiwan and the migration of the Kuroshio. *Continental Shelf Research*, **20**, pp. 349–371.

TOKESHI, R., ICHIKAWA, K., FUJII, S., SATO, K. and KOJIMA, S., 2007, Estimating the geostrophic velocity obtained by HF radar observations in the upstream area of the Kuroshio. *Journal of Oceanography*, **63**, pp. 711–720.

YANG, Y., LIU, C.-T., HU, J.-H. and KOGA, M., 1999, Taiwan current (Kuroshio) and impinging eddies. *Journal of Oceanography*, **55**, pp. 609–617.

ZHANG, D.X., LEE, T.N., JOHNS, W.E., LIU, C.-T. and ZANTOPP, R., 2001, The Kuroshio east of Taiwan: Modes of variability and relationship to interior ocean meso-scale eddies. *Journal of Physical Oceanography*, **31**, pp. 1054–1074.